A unified approach to thermo-mechano-caloric-characterization of elastocaloric materials

Journal of Physics: Energy

PAPER

A unified approach to thermo-mechano-caloric-characterization of elastocaloric materials

Franziska Louia[1,*], Nicolas Michaelis[2], Andreas Schütze[3], Stefan Seelecke[1] and Paul Motzki[1,4]

[1] Intelligent Material Systems Lab, Department of Systems Engineering, Department of Materials Science and Engineering, Saarland University, Saarbrücken, Germany
[2] HYDAC Fluidtechnik GmbH, Sulzbach/Saar, Germany
[3] Lab of Measurement Technology, Saarland University, Saarbrücken, Germany
[4] Center for Mechatronics and Automation Technology—ZeMA gGmbH, Saarbrücken, Germany
* Author to whom any correspondence should be addressed.

E-mail: franziska.louia@imsl.uni-saarland.de

Keywords: elastocaloric effect, superelastic, NiTi, experimental, latent heats, load-dependency

OPEN ACCESS

RECEIVED
24 April 2023

REVISED
13 July 2023

ACCEPTED FOR PUBLICATION
19 September 2023

PUBLISHED
13 October 2023

Abstract

This paper presents a novel approach to characterizing the relevant mechanical, thermal and caloric properties of elastocalorics material in a single testing device. Usually, tensile experiments are performed to determine the rate- and process-depending stress/strain behavior of nickel-titanium-based shape memory alloys and potentially other elastocaloric materials made from metallic alloys. These tests are relevant for, e.g., characterization of hysteresis properties and subsequent calculation of mechanical work input. In addition, simultaneous observation with an infrared camera is useful to understand temperature evolution and maximum temperature changes achievable during the loading/unloading process. Characterization of the caloric properties of the materials determines latent heats and, together with the mechanical work, also the material coefficient of performance. It is typically carried out via differential scanning calorimetry (DSC), which is performed in a separate device and requires a second experiment with different types of samples. Furthermore, DSC measurements do not reflect the way mechanically induced phase transformations trigger the release and absorption of latent heats as it is the case for elastocalorics. In order to provide a more consistent understanding of the relevant elastocaloric material properties, we here present a novel method that (a) allows for a systematic determination of load-dependent latent heats and (b) introduces a comprehensive testing setup and suitable testing routine to determine the mechanical, thermal and caloric parameters in the same experimental device and with the same sample, thus greatly simplifying the overall procedure.

1. Introduction

The increasing global demand for climatization systems will require extremely large amounts of energy in the future. The International Energy Agency estimates the energy required for space cooling and air conditioning alone to increase to more than 30% of the global energy consumption by 2050 [1]. Furthermore, conventional climatization techniques rely on environmentally harmful carbon-based refrigerants with undesirable properties such as flammability [2]. In the course of this development, it is of great importance to find and advance energy-efficient and environmentally friendly alternatives to conventional climate conditioning technologies. Amongst the many interesting alternatives, the EU Commision and the US Department of Energy have identified elastocalorics technology as the most promising alternative [3, 4], but, to date, the development of optimized elastocalorics materials is still in its infancy, and there is no commercially available material on the market yet.

The elastocaloric effect is based on the release and absorption of latent heats during mechanical loading and unloading of a suitable material. There are several, mostly metal-based materials exhibiting this effect,

such as copper-based or ferrous shape memory alloys (SMA) [5]. Superelastic SMAs made from nickel-titanium (NiTi) alloys currently provide the most promising properties concerning their thermo-mechano-caloric behavior [6]. This potential, however, is based on existing materials, which were mainly developed for use in the medical sector. Further development of specific elastocaloric alloys is necessary and will require a systematic and efficient characterization approach, crucial for evaluation and comparison of different alloy compositions and their relevant elastocaloric properties [7–10].

As a superelastic NiTi SMA is loaded, a stress-induced exothermic first-order phase transformation from austenite to martensite takes place, releasing latent heats and heating the material. During mechanical unloading, the reverse endothermic transformation from martensite to austenite occurs, leading to the absorption of latent heats from the environment and a decrease of temperature [11].

Several works have shown the potential of NiTi-based alloys [11–21]. With a suitable overall elastocaloric system and an optimized material, temperature changes of up to $\pm$30 K are possible with currently available materials [22]. At the same time, due to the small amount of mechanical work input required, a coefficient of performance (COP) of up to 30 could be demonstrated, which is many times higher than with conventional vapor compression technologies [23].

In the development process of elastocaloric climatization systems [24–28], the characterization of the existing materials plays a major role in order to investigate material parameters and to determine the mechanical and thermal behavior of the material in future applications [29].

Therefore, a number of different experiments and suitable testing devices are needed. Basic mechanical characterization of NiTi alloys is widely common and partly already carried out by material providers. When it comes to specific thermal and caloric investigation of materials with regard to elastocaloric applications, there is still a lack of experimental data and experimental test setups. Most of all, the caloric investigations of latent heats are typically done by differential scanning calorimetry (DSC), which requires special testing devices and a different sample size and preparation of material than it is used for mechanical or thermal characterization [30]. Also, results obtained by DSC are not suitable to predict the behavior of materials undergoing mechanical stress input in applications. Thus, new ways of material investigation in very few steps with little effort and building up knowledge about material behavior under application conditions is highly required.

Additionally, due to the strong thermo-mechanical coupling in SMAs, all material parameters are dependent on each other and influenced by loading and environmental conditions, e.g. a strong dependence of mechanical and thermal behavior on maximum applied strain or strain rate of mechanical loading exists [31]. Similarly, the amount of latent heats released depends on the maximum applied strain [32].

The aim of this work is to introduce a comprehensive testing device, which allows performing mechanical, thermal and caloric characterization of materials under application conditions in one setup and with the same sample by implementing a new experimental way to determine latent heats rather than by DSC. Also, a testing routine is proposed to systematically characterize the relevant properties of superelastic NiTi wires. This systematic measurement routine is a first approach to developing future standards for experimental characterization of elastocaloric materials. In the course of the recent ELASTOCALORICS2023, the first conference dedicated solely to elastocalorics, the International Elastocaloric Society was founded, aiming amongst others at standardization of experimental techniques and furthering of material development [33].

2. Key properties of elastocaloric materials

Along with climate-friendly operation, the key feature of elastocalorics technology is its energy efficiency.

2.1. COP

This efficiency is based on the so-called material COP_{mat}, which is calculated by the ratio of released or absorbed latent heat H and mechanical work input W during a loading/unloading cycle, see equation (1) [34].

$$COP_{\mathrm{mat}} = \frac{H}{W}. \tag{1}$$

If one wants to determine the suitability of a given material for elastocalorics applications, it is hence important to experimentally characterize the following quantities:

2.2. Mechanical work

The elastocalorically most relevant mechanical work input is given by the area of the mechanical stress/strain hysteresis. In addition, the value of plateau stresses and the resulting width of hysteresis are important features impacting the design of elastocaloric systems. These properties depend on a number of factors that need to be accounted for by systematic stress/strain experiments. Clearly, they vary from one material to another, but they also depend on loading conditions, e.g., strain rate and strain increment. Furthermore, material training carried out before application also has been shown to have a strong influence and needs to be characterized.

2.3. Latent heats

The latent heats released during mechanical loading and absorbed during unloading are essential for the potential heating and cooling powers of elastocaloric materials. High latent heats in materials lead to higher COPs, but they also determine the maximum temperature span during elastocaloric cycling [35]. From an experimental point of view, it is important for elastocalorics to account for, e.g., the load-dependencies of latent heats and the amount of latent heats due to application-specific partial transformations.

2.4. Temperatures

In addition to the efficiency-motivated work and heats, the observation of material temperatures during loading and unloading is of relevance because these temperatures constitute the basis for efficient heat transfer to an ambient medium, which is to be cooled or heated. Here, experimental aspects to be taken into account are, e.g. strain-rate dependency, adiabatic (max. and min.) temperature span, and also the homogeneity of temperature profiles.

From the above, it can be concluded that an assessment of a material's elastocaloric potential hence requires

- **mechanical**,
- **thermal**, and
- **caloric** characterization.

In particular due to the strong coupling of these effects and in order to account for elastocalorically relevant loading scenarios, it is desirable to perform these experiments in one setup while ideally using the same specimen. In the sequel, we will give a brief review of how the subject is currently being addressed, and then propose a novel method to characterize elastocaloric materials in a unified way.

3. Characterization of elastocaloric materials—I: integrated comprehensive testing device

In this work, we focus on the characterization of NiTi wire samples in tension loading, but the ideas also apply to other sample and loading types. Some examples are thin films [36, 37], dog-bone shaped samples with bigger dimensions [38], sheets [39] or tubes [40]. Ambient conditions also play an important role in characterizing elastocaloric materials, ranging from ambient temperatures in unclimatized laboratories to enclosed temperature-controlled testing chambers.

Regardless of the above variations, uniaxial tensile testing to determine mechanical properties of materials is the most commonly performed test. It can be carried out with commercially available axial servo-hydraulic testing systems [35, 38, 41], but custom-built test setups, like the comprehensive setup described in this work, have also been reported, see, e.g. [42, 43]. Characterization of stress/strain hysteresis in terms of plateau stresses, hysteresis width and area are the mechanically relevant quantities typically extracted after testing.

Occasionally, the use of temperature chambers has been reported as additional setup for measurements [35, 41, 43]. Unfortunately, there is no simple way of performing infrared (IR) imaging inside these chambers, so there typically is a lack of thermal information during these tests. For thermal characterization, IR imaging is the most useful method to analyze temperature evolution in elastocaloric materials. Sometimes, thermal characterization is performed by using thermocouples attached to the material [35]. However, this method does not provide spatial resolution in terms of transformation fronts throughout the wire but is able to measure temperature peaks at fixed sample locations. It should be noted, that temperature measurement by thermocouples is also not feasible for thin wire material, as attachinging thermocouples to the wire surface is introducing non-negligible heat sinks.

Together with IR measurements, digital image correlation has also been used to map the correlation between strain distribution over sample length and width and the temperature measured [15, 41, 42]. These

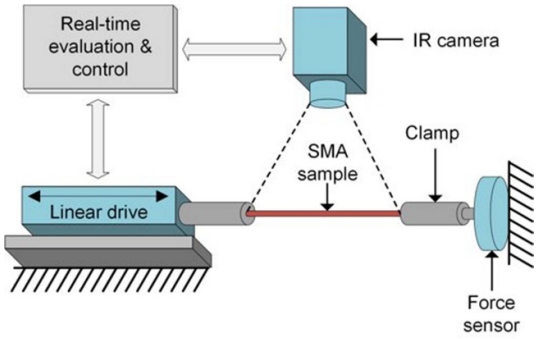

Figure 1. Schematic illustration of elastocaloric test setup for mechanical and thermal characterization [46]. Reproduced from [46]. Adapted from [47] with permission from Springer Nature.

experiments are not stringently necessary for elastocalorics, but can provide additional information on the homogeneity of transformation [17, 42].

There is one common aspect of all reported test setups, independent of sample shape or size, the determination of latent heats is consistently performed by DSC measurements, see [15, 41–44]. However, caloric data collected by DSC are the result of temperature-controlled heating and cooling of samples under zero-load conditions. This neither accounts for the load-induced trigger mechanism of elastocaloric phase transformations, nor does it capture the potential load-dependence of the latent heats themselves. Furthermore, it requires a separate device, such that caloric characterization is not part of of the thermal and mechanical characterization, and hence it does not reflect the inherent coupling between the material properties.

In the following, we introduce a device and suggest a set of potential measurements as a first step towards systematic and coherent characterization of relevant elastocaloric material properties.

3.1. Mechanical and thermal characterization

A custom-built testing device tailored for experimental investigation of superelastic NiTi materials has been developed in [31, 45].

For the mechanical characterization, it uses a linear drive (Esr-Pollmeier-LM1418), with a load maximum of 1200 N, a maximum strain rate of 1 s^{-1} and a maximum stroke of 280 mm. With an internal position decoder, a load cell (ME-Meßsysteme, KD40s) and a National Instruments CompactRIO real time data acquisition system running LabVIEW 2017, it allows for a large range of wires with different diameters to be tested from slow and isothermal to fast and adiabatic conditions. A particular custom-designed clamping mechanism enables quick exchange of various wires, while ensuring uni-axial alignment.

In order to monitor the temperature evolution during the loading/unloading processes of superelastic NiTi wires, a high-resolution IR camera system is installed as part of the test setup, see figure 1.

The IR camera (Infratec, model IR 8380) is capable of measurements with a resolution of 0.1 K and a sample rate of up to 200 Hz when focused on the wire length, so even minor changes in temperature can be determined [48]. Prior to testing, the wire surface needs to be coated with a black paint providing an emission coefficient of 0.95 to enable quantitative measurements [49]. In order to visualize thermograms of distinct cycles, temperature data are extracted and subsequently averaged from pixels in a box around the wire.

3.2. Caloric characterization

Usually, caloric characterization of materials is carried out by DSC measurements [50]. A DSC device simultaneously heats and cools two small identical furnaces under temperature control. One of the furnaces is filled with a sample of the material under investigation, the other one is empty and serves as reference. Measuring the differential heat flux between the furnaces, one can determine specific heats and-during temperature-triggered phase transformations-also the associated latent heats along with start and finish temperatures of the transformations [44]. This is the standard way to investigate the behavior of, e.g., thermally- driven SMA actuators, with a thermally-induced, load-free transformation from twinned martensite to austenite. The elastocaloric effect, on the other hand, is triggered by the application and removal of mechanical loads and not by temperature changes. Furthermore, DSC measurements do not account for stress-induced transformation between austenite and detwinned martensite.

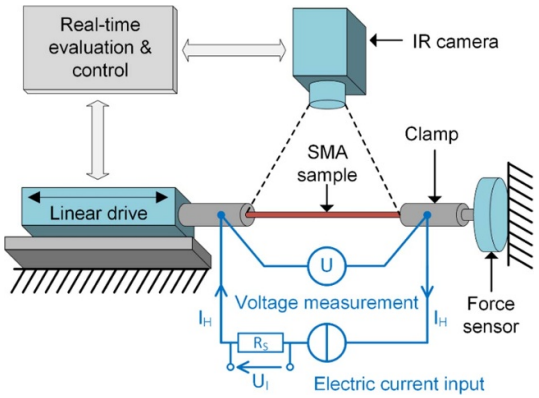

Figure 2. Schematic illustration of the elastocaloric test setup for additional caloric characterization. Reproduced from [51], with permission from Springer Nature.

Also, latent heats and thermal output of the effect are typically dependent on the level of applied loads, which is also not captured by load-free DSC measurements. For these reasons, we subsequently suggest a method that can be integrated into the above device for thermo-mechanical characterization, and hence presents a number of advantages for the elastocaloric characterization of superelastic materials.

This novel approach is based on the idea of reproducing the exothermic temperature effects of the sample under loading by a direct Joule heating of the wire. After recording the temperature change during loading, a constant-amplitude electric current of the same duration as the loading process is applied to the wire. This leads to an increase in temperature, which will be simultaneously observed by the installed IR camera. The electrically induced temperature change is then matched with the elastocaloric temperature change by adjusting the electric power amplitude passing through the wire in an iterative process. Power amplitude and pulse duration subsequently allow for a quantitative determination of the energy during the process, which is a very good approximation to the latent heats from the mechanical loading process [46, 51].

To induce electric current and to measure the electric power input the former mechanical test setup is extended as shown in figure 2. A custom-built current source provides the current I_H to perform Joule heating. A resistor, R_S, is incorporated to account for the current-dependent voltage U_I. Additionally, a voltmeter is added to the setup to measure the voltage drop U_C over the investigated wire sample.

Based on the electric parameters, the total electric power can be calculated according to equation (2). R_C stands for the total resistance of the clamps that needs to be taken into account. The value of R_S is chosen to be $R_S = 0.22\ \Omega$, the value of R_C is measured as $R_C = 20\ m\Omega$ [51].

$$P_W = I_H \cdot U_C - I_H^2 \cdot R_C = \frac{U_I}{R_S} \cdot U_C - \left(\frac{U_I}{R_S}\right)^2 \cdot R_C. \tag{2}$$

As the procedure described above works very well for the loading-induced exothermic release of latent heats, the same Joule heating method obviously cannot be used to simulate the cooling of the wire as it happens during mechanical unloading. Therefore, in this case, mechanical unloading and Joule heating are performed simultaneously with the electric heat pulse used to compensate the endothermic temperature decrease due to the elastocaloric effect. The correct amount of Joule heating is determined by the criterion that the temperature level at the end of the unloading process is the same as at the start.

For both cases, loading and unloading alike, the specific latent heat Δh of the material can then be calculated according to equation (3), with m being the mass of the investigated SMA wire.

$$\Delta h = \frac{P_W \cdot t_{\mathrm{Pulse}}}{m}. \tag{3}$$

It is particularly important to point out that the above integration into the thermo-mechanical testing device allows for elastocaloric characterization in one single device with one sample. The device can also account for the effects of different sample geometries, i.e wire diameter or other shape factors for different sample types, as well as partial, application-oriented loading typically encountered in machines.

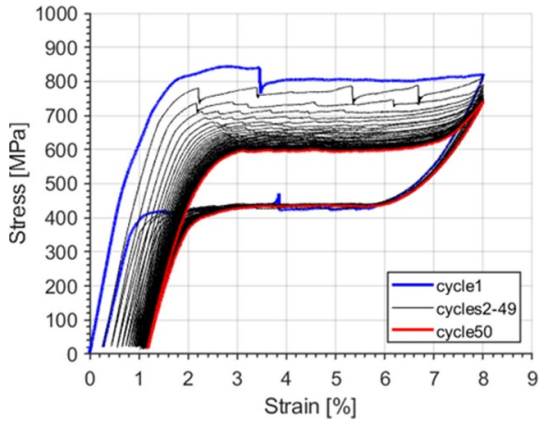

Figure 3. Stress/strain behavior during 50 cycles (1st: blue, 50th: red) of training with 8% maximum strain and 5×10^{-3} s^{-1} strain rate, wire diameter of 200 μm and free length of 90 mm, material: NiTi#3.

4. Characterization of elastocaloric materials—II: method and experimental validation

In this section, we would like to give a few examples of elastocalorically relevant characterization scenarios. In the future, these may lead to a systematic testing routine for characterizing different materials and assessing their suitability for elastocaloric applications.

The proposed routine consists of four basic steps:

1. Training,
2. Adiabatic loading behavior,
3. Determination of latent heats, and
4. Partial loading behavior.

The different steps of the testing routine will be described in the following.

4.1. NiTi material

The focus of this work is on the validation of the described test setup and the illustration of the characterization routine. To this end, we show results with a number of different metallic materials to illustrate the variety of behaviors that can be captured. A full characterization of one particular material or the systematic study of influences of various parameters during testing will be addressed in subsequent publications.

Wire materials with diameters of 200 μm and 500 μm provided by Fort Wayne Metals, NiTi#3, and Ingpuls, binary $Ni_{50.9}Ti_{49.1}$ [52, 53], were used for the tests. Samples were consistently cut to a free length of 90 mm.

Additionally, experiments were performed on $Ni_{51.1}Ti_{48.9}$ ribbons with a cross section of 1.7 mm^2 and a free length of 90 mm in order to illustrate the possibilities of the test setup [47].

All test results shown were obtained by experiments performed in an air-conditioned room with a stationary temperature of 22 °C to ensure repeatability and comparability.

4.2. Training, mechanical hysteresis, and homogenization

There are several training-related aspects of particular relevance to elastocalorics.

For stable behavior, NiTi materials typically require a training procedure, consisting of a number of loading/unloading cycles.

The mechanical data obtained during training of NiTi#3, performed for 50 cycles with a maximum strain of 8% and a strain rate of 5×10^{-3} s^{-1} is shown in figure 3. Starting from the first cycle, a significant reduction in upper plateau stress is observed, as well as an increase of remanent strain after unloading. Over several training cycles, the shape of hysteresis also changes. The singular stress drops on the upper plateau give way to a considerably smoother behavior, and as the lower plateau stress remains at a similar level, the size of the hysteresis also decreases. It becomes clear that the necessary elastocaloric work input can be reduced significantly through training, and hence it will also have an effect on the material COP.

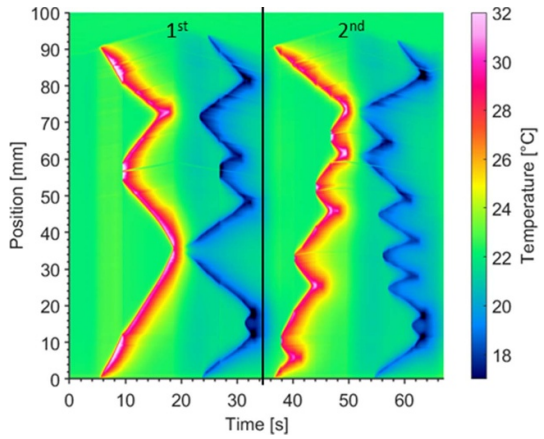

Figure 4. Thermal behavior during 1st and 2nd cycle of training with 8% maximum strain and 5×10^{-3} s^{-1} strain rate, wire diameter of 200 μm and free length of 90 mm, material: NiTi#3.

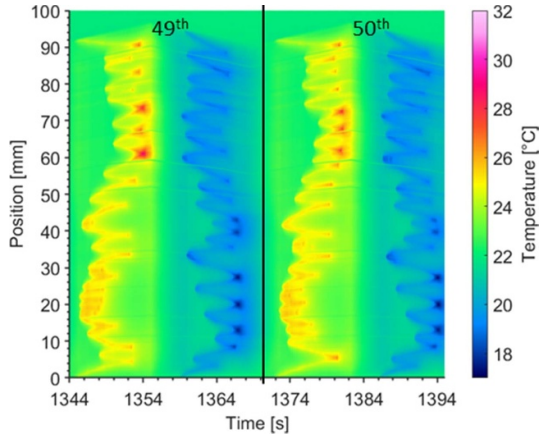

Figure 5. Thermal behavior during 49th and 50th cycle of training with 8% maximum strain and 5×10^{-3} s^{-1} strain rate, wire diameter of 200 μm and free length of 90 mm, material: NiTi#3.

However, training is not only of relevance for elastocalorics because of its effect on mechanical work. The second aspect becomes visible by inspection of IR thermograms. Here, one can clearly see individual phase fronts propagating through the wire during loading in the first cycles, see, e.g. figure 4. These phenomena are well known since the work by Shaw *et al* [54], and they are also the reason for the stress drops on the transformation plateaus. However, Schmidt *et al* [55], could show that there is a training effect of this temperature behavior as well, which manifests itself in an increasing homogenization of the phase transformation by forming more and more nucleation sites over the cycles. This explains the fact that the stress/strain hysteresis becomes smoother with increasing number of cycles, but it is also a desirable feature for elastocalorics. Figure 5 shows that the temperature evolution upon mechanical loading and unloading has become increasingly homogeneous over the cycles. This means that the heat transfer to the environment now becomes significantly more efficient because the entire wire participates in the process instead of the nucleation front location only.

Another aspect that is noteworthy here is the difference in elastocaloric behavior due to different wire geometries and different training parameters. While figures 4 and 5 showed the behavior of a 200 μm wire, figure 6 shows the temperature evolution for a thicker wire of the same material, resulting in complete thermal stabilization during the training procedure of a NiTi#3 wire with a diameter of 500 μm [55]. The training procedure consists of 100 cycles with a maximum strain of 9% and a strain rate of 1×10^{-3} s^{-1}. Distinct transformation fronts are visible during the 1st and 5th cycle, but after 100 cycles of training, shown in figure 6(c), they have completely disappeared, and the wire exhibits a very homogeneous distribution, optimally suited for heat transfer to, e.g. surrounding air or fluid. Also, the homogenization can be seen in other sample geometries, like displayed for ribbon samples in [55].

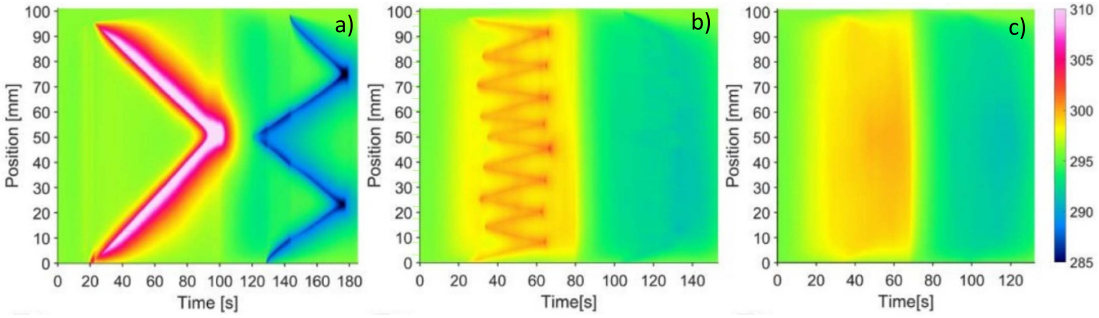

Figure 6. Evolution of thermal behavior in (a) 1st cycle, (b) 5th cycle and (c) 100th cycle of training with 9% maximum strain and 1×10^{-3} s^{-1} strain rate, temperature scale given in Kelvin belonging to (a)–(c), wire diameter of 500 μm and free length of 90 mm, material: NiTi#3. Reproduced from [56]. © IOP Publishing Ltd. All rights reserved.

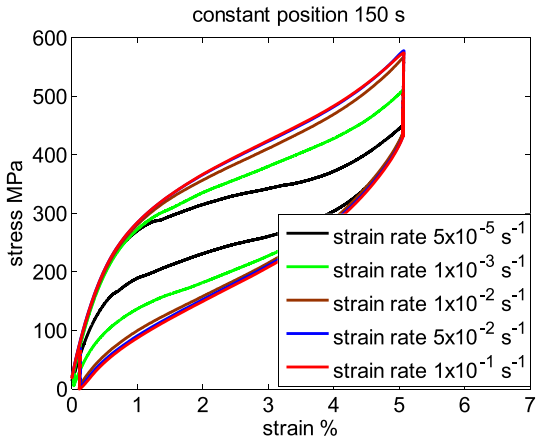

Figure 7. Stress/strain behavior for different strain rates, indicating effect on hysteresis shape and resulting work input, ribbon with cross section of 1.7 mm^2 and free length of 90 mm, material: $Ni_{51.1}Ti_{48.9}$. Reproduced with permission from [31].

4.3. Adiabatic loading

Once the material is trained, it is exposed to adiabatic loading conditions. These are relevant for elastocalorics, because they lead to the largest possible temperature changes.

Before conducting specific experiments, adiabatic strain rates for the specific samples need to be identified by mechanical and thermal investigation. Figure 7 shows the change in mechanical behavior of $Ni_{51.1}Ti_{48.9}$ ribbon samples with increasing strain rates from 5×10^{-5} s^{-1} up to 1×10^{-1} s^{-1} due to the thermomechanical coupling. The faster the strain rate, the less time the ribbon has for heat exchange with the environment, leading to a saturation behavior in the adiabatic limit [47]. In order to subsequently ensure a full exchange of released latent heats with the environment, the constant position after loading and unloading, respectively, is held for 150 s.

It can be seen that shape and slope of hysteresis change for different applied strain rates. Furthermore, the resulting work input is increasing with increasing strain rate. Simultaneously performed thermal characterization shows the dependency of temperature peaks in relation to different strain rates, as displayed in figure 8. At about the rate of 5×10^{-2} s^{-1}, the temperature increase and decrease in the material is saturating around 20 K. Increasing the strain rate to 1×10^{-1} s^{-1} does not increase the temperature change any further, and the mechanical hystereses displayed in figure 7 are no longer distinguishable, hence the adiabatic limit is reached.

4.4. Latent heats

In order to investigate the efficiency of elastocaloric materials, latent heats also need to be determined along with the mechanical work from the hysteresis area. The measurements shown in the following were performed using the novel method introduced above.

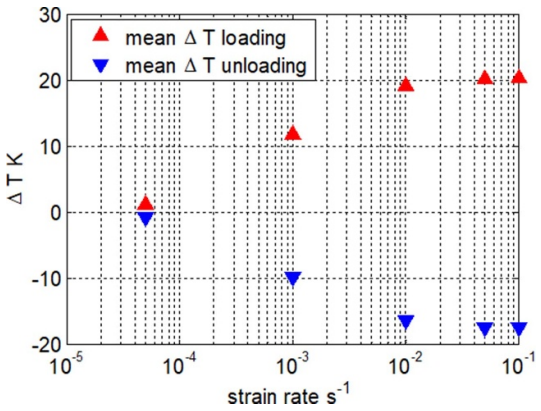

Figure 8. Relation of temperature peaks on applied strain rates to determine adiabatic elastocaloric behavior, ribbon with cross section of 1.7 mm^2 and free length of 90 mm, material: $Ni_{51.1}Ti_{48.9}$. Reproduced with permission from [31].

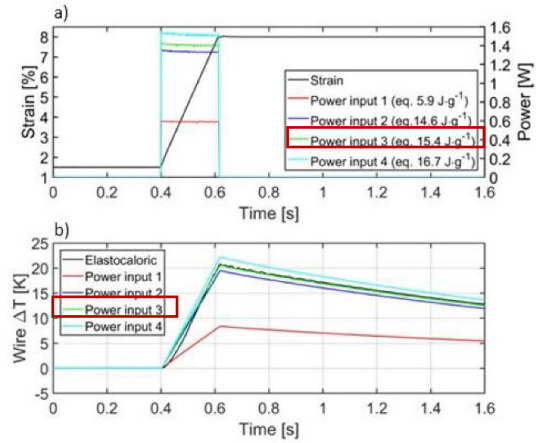

Figure 9. Determination of latent heat during loading process with complete austenite to martensite transformation, (a) mechanical strain (black) and power of heating pulse (colored) over time for loading process, (b) comparison of elastocaloric temperature change (black) and electric induced temperature change (colored) during loading, wire diameter of 200 μm and free length of 90 mm, material: NiTi#3. Reproduced with permission from [46].

Figure 9 illustrates the experimental procedure to determine the latent heat during loading of NiTi#3 with a maximum strain of 6.5%, covering complete phase transformation [46]. In figure 9(a), (upper part), mechanical strain (black) and different applied electric power pulses (colored) are displayed over time.

The lower part, figure 9(b) displays the temperature change of the sample due to elastocaloric loading (black) and the resulting temperature changes during applied power pulses (colored).

During the experiment, four different electric power inputs were used to match the elastocaloric temperature change. The temperature variation from different electric power inputs clearly shows the amplitude of the red curve to be chosen too low and the light blue too high. The green curve perfectly matches the one from the mechanical loading experiment, and the corresponding latent heat for the investigated NiTi#3 in figure 9 can be determined as $h_{A\rightarrow M} = 15.4\ J\ g^{-1}$.

In the next step, this procedure is repeated for the unloading process, shown in figure 10. Figure 10(a) again displays the mechanical strain (black) and different applied power pulses (colored) while (b) displays the comparison of elastocaloric temperature change (black) and the electrically induced compensation of temperature (colored).

The aim of this experiments is to compensate the elastocaloric cooling effect due the endothermic nature of the reverse martensite-austenite transformation. If the applied electric pulse power is not sufficient, see the red curve in figure 10(b), the temperature after the experiment is lower than the start temperature, and we observe a subsequent temperature increase until equilibrium with the environment is reached. On the other hand, application of overly high-power values leads to too high a temperature after unloading, and the reverse equilibration takes place, as the light blue curve shows. The correct power can be identified from end

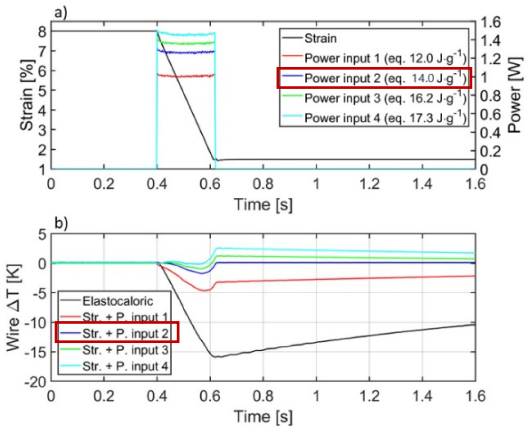

Figure 10. Determination of latent heat during unloading process with complete martensite to austenite transformation, (a) mechanical strain (black) and power of heating pulse (colored) over time for loading process, (b) comparison of elastocaloric temperature change (black) and electric induced temperature compensation (colored) during unloading, wire diameter of 200 μm and free length of 90 mm, material: NiTi#3. Reproduced with permission from [46].

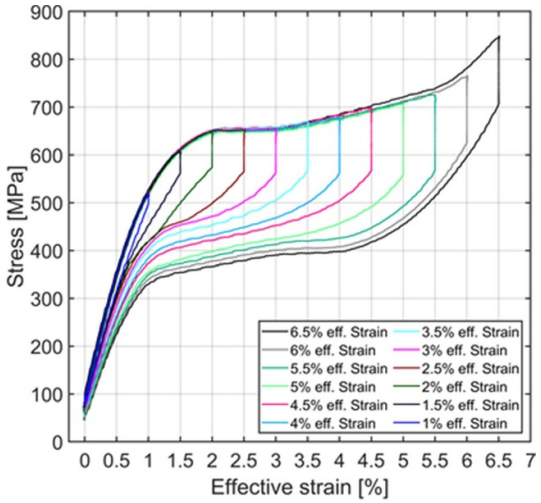

Figure 11. Stress/strain behavior for a series of partial unloading tests, up to a maximum of 6.5% total strain with a strain rate of 1×10^{-1} s^{-1}, wire diameter of 200 μm and free length of 90 mm, material: $Ni_{50.9}Ti_{49.1}$. Reproduced with permission from [46].

and start temperature being equal after the unloading process, shown in blue, and leads to a latent heat of $h_{M\rightarrow A} = 14.0$ J g^{-1}. Note that the latent heat due to unloading is slightly lower, which can be expected due to the lower stress level of the hysteretic reverse transformation.

As a validation, the obtained values for latent heats are compared to different published DSC-based experimental results, e.g. Frenzel *et al* [35] performed a systematic study of various NiTi-based-alloys, resulting in latent heats of 9 J g^{-1} up to 28 J g^{-1} for binary NiTi. Shaw *et al* [44] cite latent heats in a range of 15–20 J g^{-1}. Performing DSC measurements on SMA thin film material, Brüderlin *et al* [57] also measured latent heats of 15 J g^{-1}.

These examples show that the latent heats determined by the proposed joule heating method fit right into the representative range for binary NiTi.

4.5. Partial loading

In elastocaloric applications, operation parameters may vary, and it is important to understand how this affects work, heats, and efficiency. To this end, a series of partial loading experiments was performed in order to show the process-depending mechanical and thermal behavior during complete and partial transformations. Figure 11 displays the stress/strain behavior and resulting hysteresis curves of multiple tests with a strain rate of 1×10^{-1} s^{-1} performed with $Ni_{50.9}Ti_{49.1}$. The tests were performed starting from a

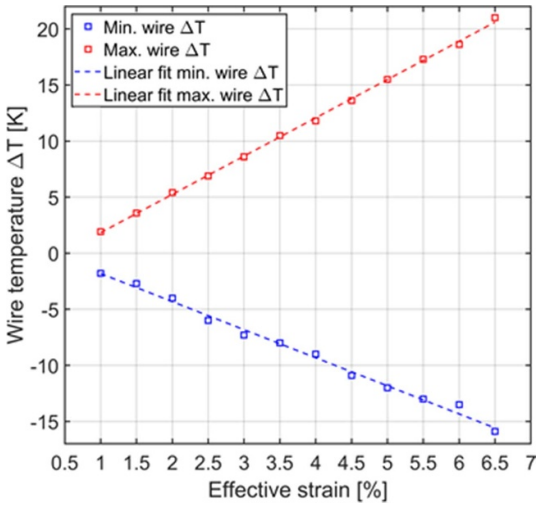

Figure 12. Maximum temperature vs. effective strain tests, from $\Delta\varepsilon = 1\%$ to a maximum of $\Delta\varepsilon = 6.5\%$ total strain with a strain rate of 1×10^{-1} s^{-1}, wire diameter of 200 μm and free length of 90 mm, material: $Ni_{50.9}Ti_{49.1}$. Reproduced with permission from [46].

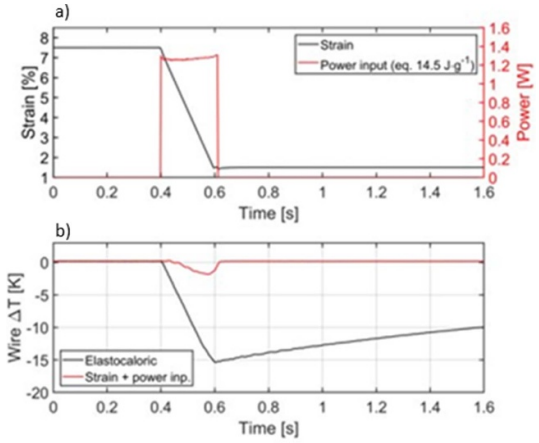

Figure 13. Determination of latent heat during unloading process with complete martensite to austenite transformation ($\Delta\varepsilon = 6\%$), (a) mechanical strain (black) and power of heating pulse (red) over time for unloading process, (b) comparison of elastocaloric temperature change (black) and electric induced temperature change (red) during unloading, wire diameter of 200 μm and free length of 90 mm, material: NiTi#3. Reproduced with permission from [46].

change in strain of 1% up to 6.5% in increments of 0.5%. After loading, a holding time of 10 s was added. The corresponding maximum temperatures prior to unloading are shown in figure 12. It can be seen that these temperatures scale linearly with the applied strain level.

In contrast to DSC measurements, the effect of partial transformation on latent heats can also be investigated with the novel test setup. Figure 13 displays the determination of latent heat on unloading with a maximum $\Delta\varepsilon$ of 6%. In comparison, figure 14 shows the process with a maximum $\Delta\varepsilon$ of 3%.

The tests performed with varying maximum strains show a decrease in released latent heat with decreasing maximum strain. For the applied $\Delta\varepsilon = 6\%$, a latent heat of $h_{M\rightarrow A,6\%} = 14.5$ J g^{-1} is observable, for $\Delta\varepsilon = 3\%$ the latent heat decreases to $h_{M\rightarrow A,3\%} = 6.8$ J g^{-1}.

Combining these results with area calculations from corresponding mechanical partial loading/unloading experiments, it will be possible to also calculate efficiencies for partial cycles and get a better estimate for machine operation under such circumstances.

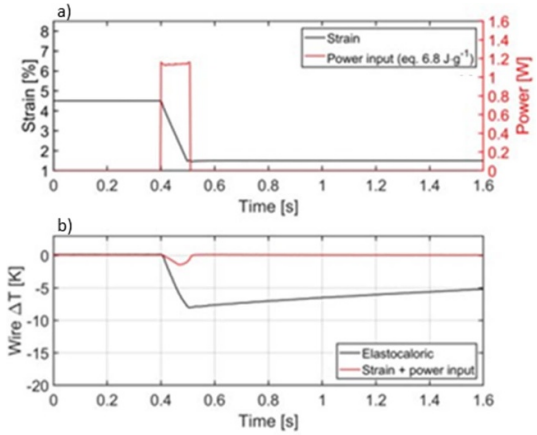

Figure 14. Determination of latent heat during unloading process with partial transformation ($\Delta\varepsilon = 3\%$), (a) mechanical strain (black) and power of heating pulse (red) over time for unloading process, (b) comparison of elastocaloric temperature change (black) and electric induced temperature change (red) during unloading, wire diameter of 200 μm and free length of 90 mm, material: NiTi#3. Reproduced with permission from [46].

5. Conclusion and outlook

This work introduced a novel comprehensive testing set up for thermo-mechano-caloric characterization of elastocaloric materials. It uses a linear drive with position encoder and load cell for mechanical testing, an infrared camera to capture temperature evolution during testing, and it introduces a novel method for the determination of load-induced latent heats, all integrated in the same device. In addition, examples of relevant experiments were shown that enable the determination of work, latent heats and hence material coefficients of efficiency (COP_{mat}) as well as maximal temperature changes achievable with materials under test. A novel feature is that it is also possible to perform partial loading tests representative for typical operating conditions in applications. An additional advantage of the integrated testing system is the fact that the complete characterization can be done on the same sample, and that it enables the determination of training effects on the elastocaloric performance of materials in a simplified way.

In future research, the determination of load-induced latent heats with the implemented method will be addressed in more detail through systematic experimental studies. In order to compare different materials and geometries, the developed characterization routine will be generalized and applied to wire material with varying cross sections as well as sheets or tubes made of different superelastic SMA. As the training behavior has already been succesfully illustrated in terms of mechanical and thermal characterization, additional caloric characterization of such training processes will contribute to further understanding of elastocalorically relevant material behavior.

Data availability statement

No new data were created or analysed in this study.

Acknowledgments

The authors gratefully acknowledge support from Fort Wayne Metals and Ingpuls GmbH for providing the NiTi wire material used in the experiments.

ORCID iDs

Stefan Seelecke https://orcid.org/0000-0003-1018-247X
Paul Motzki https://orcid.org/0000-0001-9903-2018

References

[1] OECD/IEA 2018 The future of cooling (available at: https://iea.blob.core.windows.net/assets/0bb45525-277f-4c9c-8d0c-9c0cb5e7d525/The_Future_of_Cooling.pdf)
[2] Umweltbundesamt 2017 1987-2017: 30 Jahre Montrealer Protokoll–Vom Ausstieg aus den FCKW zum Ausstieg aus teilfluorierten Kohlenwasserstoffen (available at: www.umweltbundesamt.de/publikationen/%0A1987-2017-30-jahre-montrealer-protokoll)

[3] Goetzler W, Zogg R, Young J and Johnson C 2014 *Energy Savings Potential and RD & D Opportunities for Non-Vapor-Compression HVAC Technologies* (US Department of Energy) p 3673
[4] VHK and ARMINES 2016 Commision regulation (EC) no. 643/2009 with regard to ecodesign requirements for household refrigeration appliances and commission delegated regulation (EU) no. 1060/2010 with regard to energy labelling of household refrigeration appliances (available at: www.eup-network.de/fileadmin/user_upload/Household_Refrigeration_Review_TECHNOLOGY_ROADMAP_FINAL_20160304.pdf)
[5] Moya X, Kar-Narayan S and Mathur N D 2014 Caloric materials near ferroic phase transitions *Nat. Mater.* **13** 439–50
[6] Xu Y, Lu B, Sun W, Yan A and Liu J 2015 Large and reversible elastocaloric effect in dual-phase $Ni_{54}Fe_{19}Ga_{27}$ superelastic alloys *Appl. Phys. Lett.* **106** 201903
[7] Chen H, Xiao F, Liang X, Li Z, Li Z, Jin X, Min N and Fukuda T 2019 Improvement of the stability of superelasticity and elastocaloric effect of a Ni-rich Ti-Ni alloy by precipitation and grain refinement *Scr. Mater.* **162** 230–4
[8] Lin H, Hua P, Huang K, Li Q and Sun Q 2023 Grain boundary and dislocation strengthening of nanocrystalline NiTi for stable elastocaloric cooling *Scr. Mater.* **226** 115227
[9] Shen J-J, Lu N-H and Chen C-H 2020 Mechanical and elastocaloric effect of aged Ni-rich TiNi shape memory alloy under load-controlled deformation *Mater. Sci. Eng.* A **788** 139554
[10] Hou H *et al* 2019 Fatigue-resistant high-performance elastocaloric materials made by additive manufacturing *Science* **366** 1116–21
[11] Dang P, Zhou Y, Pang J, Ding X, Sun J, Lookman T and Xue D 2023 Achieving stable actuation response and elastocaloric effect in a nanocrystalline $Ti_{50}Ni_{40}Cu_{10}$ alloy *Scr. Mater.* **226** 115263
[12] Tušek J and Pryds N 2019 Cooling with a squeeze *Physics* **12** 72
[13] Tušek J, Engelbrecht K, Millán-Solsona R, Mañosa L, Vives E, Mikkelsen L P and Pryds N 2015 The elastocaloric effect: a way to cool efficiently *Adv. Energy Mater.* **5** 1500361
[14] Lu B, Zhang P, Xu Y, Sun W and Liu J 2015 Elastocaloric effect in $Ni_{45}Mn_{36.4}In_{13.6}Co_5$ metamagnetic shape memory alloys under mechanical cycling *Mater. Lett.* **148** 110–3
[15] Pataky G J, Ertekin E and Sehitoglu H 2015 Elastocaloric cooling potential of NiTi, Ni_2FeGa, and CoNiAl *Acta Mater.* **96** 420–7
[16] Surikov N Y, Panchenko E Y, Timofeeva E E, Tagiltsev A I and Chumlyakov Y I 2021 Orientation dependence of elastocaloric effect in $Ni_{50}Mn_{30}Ga_{20}$ single crystals *J. Alloys Compd.* **880** 160553
[17] Fähler S, Rößler U K, Kastner O, Eckert J, Eggeler G, Emmerich H, Entel P, Müller S, Quandt E and Albe K 2012 Caloric effects in ferroic materials: new concepts for cooling *Adv. Eng. Mater.* **14** 10–19
[18] Takeuchi I and Sandeman K 2015 Solid-state cooling with caloric materials *Phys. Today* **68** 48–54
[19] Hou H, Qian S and Takeuchi I 2022 Materials, physics and systems for multicaloric cooling *Nat. Rev. Mater.* **7** 633–52
[20] Cui J, Wu Y, Muehlbauer J, Hwang Y, Radermacher R, Fackler S, Wuttig M and Takeuchi I 2012 Demonstration of high efficiency elastocaloric cooling with large Δt using NiTi wires *Appl. Phys. Lett.* **101** 073904
[21] Sehitoglu H, Wu Y and Ertekin E 2018 Elastocaloric effects in the extreme *Scr. Mater.* **148** 122–6
[22] Hou H, Finkel P, Staruch M, Cui J and Takeuchi I 2018 Ultra-low-field magneto-elastocaloric cooling in a multiferroic composite device *Nat. Commun.* **9** 4075
[23] Qian S, Geng Y, Wang Y, Ling J, Hwang Y, Radermacher R, Takeuchi I and Cui J 2016 A review of elastocaloric cooling: materials, cycles and system integrations *Int. J. Refrig.* **64** 1–19
[24] Kirsch S-M, Welsch F, Michaelis N, Schmidt M, Wieczorek A, Frenzel J, Eggeler G, Schütze A and Seelecke S 2018 NiTi-based elastocaloric cooling on the macroscale: from basic concepts to realization *Energy Technol.* **6** 1567–87
[25] Li X, Cheng S and Sun Q 2022 A compact NiTi elastocaloric air cooler with low force bending actuation *Appl. Therm. Eng.* **215** 118942
[26] Engelbrecht K, Tušek J, Eriksen D, Lei T, Lee C-Y, Tušek J and Pryds N 2017 A regenerative elastocaloric device: experimental results *J. Phys. D: Appl. Phys.* **50** 424006
[27] Kabirifar P, Žerovnik A, Ahčin Ž, Porenta L, Brojan M and Tušek J 2019 Elastocaloric cooling: state-of-the-art and future challenges in designing regenerative elastocaloric devices *Stroj. Vest./J. Mech. Eng.* **65** 11–12
[28] Tušek J, Engelbrecht K, Eriksen D, Dall'Olio S, Tušek J and Pryds N 2016 A regenerative elastocaloric heat pump *Nat. Energy* **1** 16134
[29] Nargatti K and Ahankari S 2022 Advances in enhancing structural and functional fatigue resistance of superelastic NiTi shape memory alloy: a review *J. Intell. Mater. Syst. Struct.* **33** 503–31
[30] Wieczorek A 2016 *Werkstoffwissenschaftliche Untersuchungen zum Kühlen mit Formgedächtnislegierungen* (Ruhr Universität Bochum)
[31] Schmidt M 2017 Elastokalorisches Kühlen mit Ni-Ti-basierten Formgedächtnislegierungen: thermodynamische Analyse, experimentelle Untersuchungen, Prozessoptimierung *PhD Thesis* Saarland University
[32] Kim Y, Jo M G, Park J W, Park H K and Han H N 2018 Elastocaloric effect in polycrystalline $Ni_{50}Ti_{45.3}V_{4.7}$ shape memory alloy *Scr. Mater.* **144** 48–51
[33] iMSL ELASTOCALORICS2023 (available at: https://imsl.de/elastocalorics2023/)
[34] Frenzel J, Eggeler G, Quandt E, Seelecke S and Kohl M 2018 High-performance elastocaloric materials for the engineering of bulk- and micro-cooling devices *MRS Bull.* **43** 280–4
[35] Frenzel J, Wieczorek A, Opahle I, Maaß B, Drautz R and Eggeler G 2015 On the effect of alloy composition on martensite start temperatures and latent heats in Ni–Ti-based shape memory alloys *Acta Mater.* **90** 213–31
[36] Chluba C, Ge W, Lima de Miranda R, Strobel J, Kienle L, Quandt E and Wuttig M 2015 Ultralow-fatigue shape memory alloy films *Science* **348** 1004–7
[37] Brüderlin F 2020 *Advanced Elastocaloric Cooling Devices Based on Shape Memory Alloy Films* (Karlsruher Institut für Technologie)
[38] Tušek J, Engelbrecht K, Mikkelsen L P and Pryds N 2015 Elastocaloric effect of Ni-Ti wire for application in a cooling device *J. Appl. Phys.* **117** 124901
[39] Tušek J, Žerovnik A, Čebron M, Brojan M, Žužek B, Engelbrecht K and Cadelli A 2018 Elastocaloric effect vs fatigue life: exploring the durability limits of Ni-Ti plates under pre-strain conditions for elastocaloric cooling *Acta Mater.* **150** 295–307
[40] Hou H, Cui J, Qian S, Catalini D, Hwang Y, Radermacher R and Takeuchi I 2018 Overcoming fatigue through compression for advanced elastocaloric cooling *MRS Bull.* **43** 285–90
[41] Wu Y, Ertekin E and Sehitoglu H 2017 Elastocaloric cooling capacity of shape memory alloys—Role of deformation temperatures, mechanical cycling, stress hysteresis and inhomogeneity of transformation *Acta Mater.* **135** 158–76
[42] Ossmer H, Chluba C, Gueltig M, Quandt E and Kohl M 2015 Local evolution of the elastocaloric effect in TiNi-based films *Shape Mem. Superelasticity* **1** 142–52

[43] Tyc O, Pilch J and Sittner P 2016 Fatigue of superelastic NiTi wires with different plateau strain *Proc. Struct. Integr.* **2** 1489–96
[44] Shaw J A, Churchill C B and Iadicola M A 2008 Tips and tricks for characterizing shape memory alloy wire: part 1—differential scanning calorimetry and basic phenomena *Exp. Tech.* **32** 55–62
[45] Schmidt M, Schütze A and Seelecke S 2015 Scientific test setup for investigation of shape memory alloy based elastocaloric cooling processes *Int. J. Refrig.* **54** 88–97
[46] Michaelis N 2020 Experimentelle Untersuchung elastokalorischer Kühlprozesse: konvektive Thermodynamik, latente Wärme und Materialzustandsüberwachung *PhD Thesis* Saarland University
[47] Schmidt M *et al Elastocaloric Cooling With Ni-Ti Based Alloys: Material Characterization and Process Variation* (*21 September 2015*) (https://doi.org/10.1115/SMASIS2015-8944)
[48] Infratec IR 8380 specifications (available at: www.infratec.de/thermografie/%0Awaermebildkameras/imageir-8300/)
[49] Tetenal Tetenal Kameralack Datenblatt (available at: https://tetenal.com/media/60/bd/3a/1605714511/351686_00_Produkt%Information_Kameralack%Spray_105202_DE_08-05-2017.pdf)
[50] Gabbott P 2008 *Principles and Applications of Thermal Analysis* (Blackwell Publishing Ltd)
[51] Michaelis N, Schütze A, Welsch F, Kirsch S-M and Seelecke S 2019 Novel experimental approach to determine elastocaloric latent heat *Shape Mem. Superelasticity* **5** 352–61
[52] FWM—Resource Library Fort wayne metals—superelastic nitinol wire (available at: www.fwmetals.com/materials/nitinol/superelastic-nitinol/)
[53] Ingpuls GmbH Produkte und Leistungen (available at: https://ingpuls.de/produkte-leistungen/)
[54] Shaw J 1995 Thermomechanical aspects of NiTi *J. Mech. Phys. Solids* **43** 1243
[55] Schmidt M, Ullrich J, Wieczorek A, Frenzel J, Schütze A, Eggeler G and Seelecke S 2015 Thermal stabilization of NiTiCuV shape memory alloys: observations during elastocaloric training *Shape Mem. Superelasticity* **1** 132–41
[56] Michaelis N, Welsch F, Kirsch S-M, Seelecke S and Schütze A 2019 Resistance monitoring of shape memory material stabilization during elastocaloric training *Smart Mater. Struct.* **28** 105046
[57] Brüderlin F, Ossmer H, Wendler F, Miyazaki S and Kohl M 2017 SMA foil-based elastocaloric cooling: from material behavior to device engineering *J. Phys. D: Appl. Phys.* **50** 424003